Article

Not peer-reviewed version

Ancient Networks in Flux: Environmental Rhythms and Human Connectivity in Arid Landscapes

[Shruti Bagde](#) *

Posted Date: 12 November 2025

doi: 10.20944/preprints202511.0803.v1

Keywords: human mobility; environmental stress; prehistoric societies; arid regions; geoclimatic reconstruction; archaeological site distribution; hydrological variability; interaction networks; climatic adaptation; sociocultural dynamics

 doi:10.20944/preprints202511.0803.v1

Article

Ancient Networks in Flux: Environmental Rhythms and Human Connectivity in Arid Landscapes

Shruti Bagde

Independent Researcher, USA; shrutibagde1617@gmail.com

Abstract

This study investigates how fluctuations in long-term environmental water availability shaped patterns of human interaction and mobility in prehistoric arid regions. Using a combination of geoclimatic reconstructions and archaeological site distributions, we analyze the relationship between climatic stressors and evolving sociocultural connections. The findings reveal dynamic shifts in regional affiliations corresponding with periods of drought and ecological stress, highlighting a strong interplay between hydrological variability and human behavioral adaptation. By examining interaction networks over time, this work offers a novel perspective on how environmental forces influenced communal strategies in ancient societies facing climatic uncertainty.

Keywords: human mobility; environmental stress; prehistoric societies; arid regions; geoclimatic reconstruction; archaeological site distribution; hydrological variability; interaction networks; climatic adaptation; sociocultural dynamics

---

1. Introduction

Human societies often develop networks of exchange to mitigate risks in unpredictable environments [1]. These social and infrastructural connections are shaped by both physical geography and environmental variability. Studies have shown that distance, climate, and sociocultural factors collectively influence the nature and strength of interaction networks [2–9]. For communities in arid zones, fluctuations in hydroclimate—particularly in precipitation and evapotranspiration—can incentivize longer-distance interactions to access diverse ecological zones [10,11]. Given the challenges in observing such dynamics over contemporary timeframes, archaeology provides a valuable long-term perspective.

Archaeological research uniquely addresses how human-environment interactions evolve, not just through physical infrastructure like canals or roads, but also via artifacts such as ceramics and trade goods. These materials offer insight into the structure and extent of past exchange systems [12]. However, connecting these material traces with environmental patterns is often difficult due to limitations in both the archaeological and paleoclimate records.

The American Southwest stands out as an exception, where extensive archaeological data and high-resolution climate reconstructions coexist [13–22]. This region reveals well-preserved social networks marked by ceramic and obsidian trade, and episodes of transformation linked to severe droughts [23–27]. Despite earlier efforts to explore climate-society linkages, data limitations hindered detailed analysis [10,28]. Recent advances now allow for more precise exploration of these relationships [29,30].

This study investigates how long-term drought patterns influenced social connectivity in the late pre-Hispanic US Southwest. Treating social networks as dynamic systems, I use principal components analysis to identify dominant drought patterns and compare them with archaeological ceramic distributions—proxies for social interaction. Results show that while interaction diminishes with distance, it strengthens between regions experiencing contrasting climate regimes. This research contributes to a more nuanced understanding of how environmental forces shaped ancient human networks.

 doi:10.20944/preprints202511.0803.v1

2. Data and Methods

2.1. Hydroclimate Variability

Understanding the societal impact of drought requires separating meaningful climatic signals from background variability. While Principal Components Analysis (PCA) is a widely used method in climate science to extract dominant modes of variability [31,32], its application in archaeology remains limited [28,33]. In this study, PCA was employed to analyze a 100-year dataset of 12-month Standardized Precipitation-Evapotranspiration Index (SPEI), calculated for August to reflect critical agricultural conditions. The dataset spans Arizona, New Mexico, Colorado, Utah, and California, derived from interpolated weather-station data [34,35].

The resulting empirical orthogonal functions (EOFs) were obtained by decomposing the space-time covariance matrix using singular value decomposition. Grid cells were weighted by the cosine of latitude to address areal distortion. Key eigenvalues were selected through a scree plot and North's rule of thumb [36], and then rotated using varimax transformation to highlight coherent spatial structures [37]. Each EOF represents a distinct spatial pattern, while their corresponding principal components (PCs) capture temporal variability. Correlation signs were standardized for interpretability. To ensure consistency over time, the EOFs were validated against long-term SPEI reconstructions [38].

2.2. Archaeological Interaction Networks

The Southwest Social Networks (SWSN) database aggregates cultural material data from approximately 1,000 well-dated archaeological sites across Arizona and New Mexico [25,30,39–42]. It includes around 4.7 million ceramic and 5,000 obsidian artifacts. To mitigate biases due to settlement aggregation, the point-based data were transformed into 10 km grid cells [43].

To quantify interaction strength, the modified Jensen-Shannon divergence was computed between the frequency distributions of 15 decorated ceramic types across each grid cell pair:

$$D_{ij} = H(\pi_1 P + \pi_2 Q) - \pi_1 H(P) - \pi_2 H(Q), \tag{1}$$

where D_{ij} denotes divergence between sites i and j, $H(P) = -\sum_i p_i \ln_2 p_i$ is Shannon entropy, and $\pi_1 = \pi_2 = 0.5$ represent equal weighting. This metric serves as a proxy for the probability of social interaction, reflecting shared or divergent ceramic usage patterns [44].

2.3. Least-Cost Path Networks

Physical distance plays a critical role in limiting social interactions by increasing time, effort, and resource costs. These constraints also affect migration feasibility, partner selection, and transportation costs [2,45,46]. To account for geographic impedance, a least-cost path network was constructed using a 90m Shuttle Radar Topography Mission (SRTM) DEM resampled to 250m.

Movement costs between adjacent cells were calculated based on Tobler's hiking function, modified for isotropy and penalization on steep terrain [47]. The resulting time-based cost matrix was inverted to model conductance, and least-cost paths were computed between all occupied 10 km grid cells using efficient graph algorithms [48].

2.4. Spatial Interaction Modeling

Spatial interaction models estimate the intensity of flows—such as people, goods, or ideas—based on factors influencing origin-destination dynamics and separation costs [49–54]. Though rarely applied statistically in archaeology due to sparse data [55–57], these models align conceptually with approaches in molecular ecology and cultural transmission studies [53,58].

Challenges in modeling include bounded and symmetric pairwise data, and a lack of theoretical guidance for specifying functional forms. To accommodate this, generalized additive models (GAMs) were used [59], enabling flexible estimation via penalized splines [60].

The fitted model is defined as:

Preprints.org (www.preprints.org) | NOT PEER-REVIEWED | Posted: 12 November 2025 doi:10.20944/preprints202511.0803.v1

$$\text{logit}(D_{ijt}) = f(\text{dist}_{ij}) + f_t(\text{EOF}_{ij}) + \tau_{it} + \tau_{jt} + \epsilon_{ijt}, \tag{2}$$

where dist_{ij} is the least-cost distance, EOF_{ij} represents climatic dissimilarity, τ are time-varying random effects capturing node-level variability, and ϵ is Gaussian error. Model comparison using AIC, BIC, and R^2 evaluated the significance of adding climate-based predictors. The final model was re-estimated using restricted maximum likelihood to improve fit [61,62].

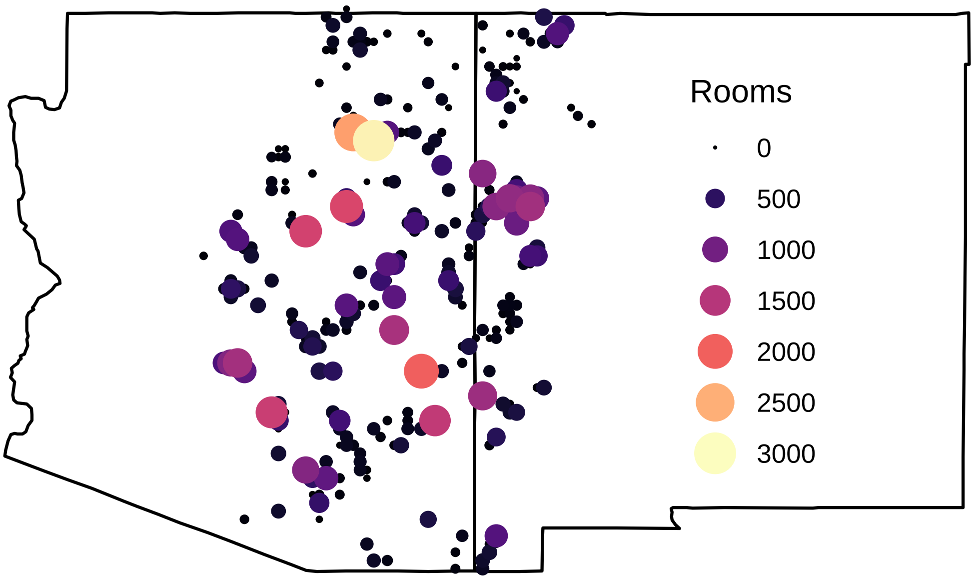

Figure 1. The *Southwest Social Networks* dataset, version 1. (TODO more detail and include network figures here?)

3. Results

3.1. Dominant Drought Modes Capture the Majority of Climate Variability

An analysis of the principal components derived from the 100-year Standardized Precipitation-Evapotranspiration Index (SPEI) record reveals that the six most significant temporal modes account for approximately 83% of the total variance observed across the dataset (Figure 2). These principal components (PCs) summarize the most influential temporal trends in drought intensity and duration across the American Southwest. To improve interpretability and reduce statistical noise, the top six components were subjected to varimax rotation before being mapped. This process enhances the physical coherence of the spatial patterns linked to each component, while omitting subsequent PCs that exhibit lower explanatory power and increased sampling variability. The choice to limit the analysis to six components reflects a balance between maximizing explained variance and avoiding the inclusion of degenerate or spatially incoherent patterns.

 doi:10.20944/preprints202511.0803.v1

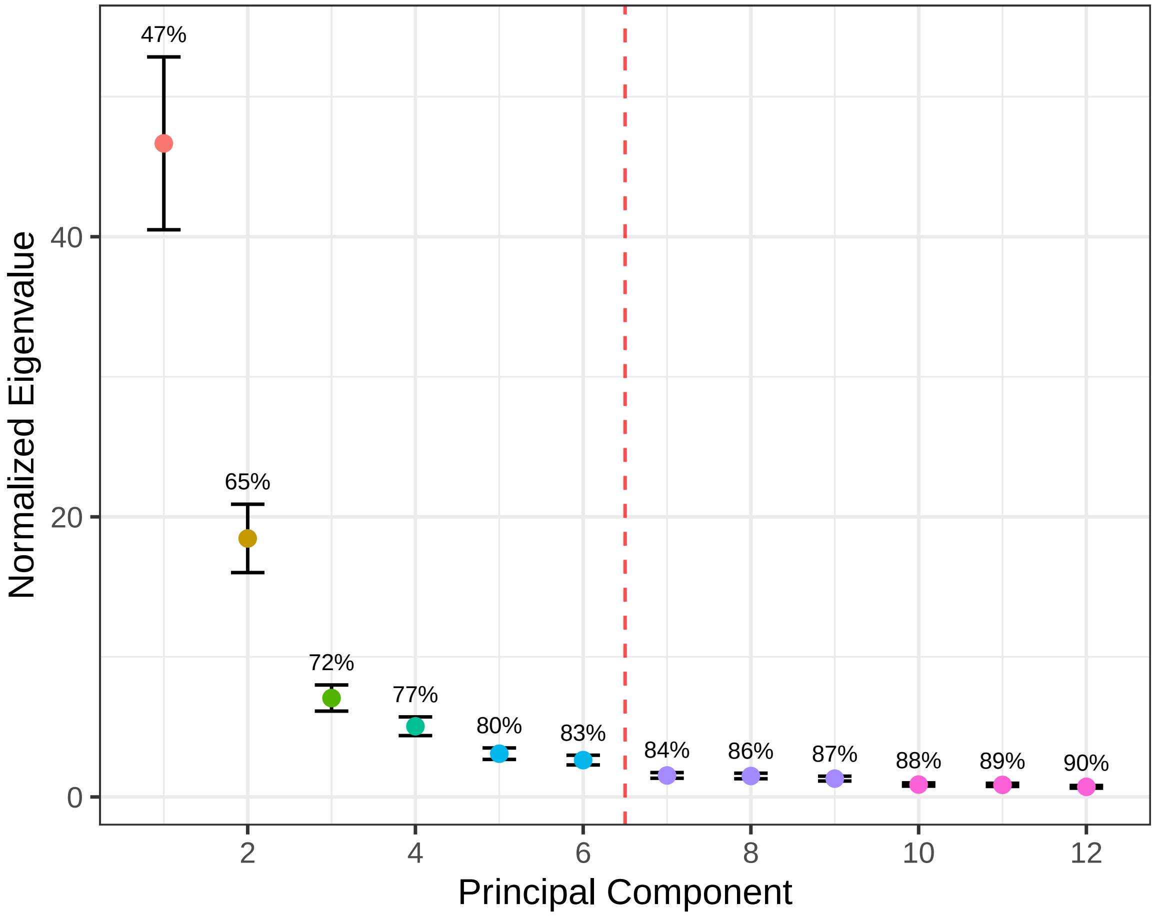

Figure 2. Leading 12 principle components, in order of decreasing eigenvalues, along with the cumulative percent of the variance explained by the leading PCs. Standard errors calculated using North et al.'s rule of thumb [36]. PC's with the same colors (5-6, 7-9, 10-12) are degenerate multiplets, meaning they cannot be clearly distinguished from one another given the sampling variability in the observational dataset. The dashed line represents the truncation point, beyond which PCs were not retained for further analysis. The leading 6 PCs collectively explain 83% of drought variability in the observed drought record.

3.2. Spatial Drought Patterns Reflect Distinct Climate Forcings

The spatial signatures associated with the leading PCs, or empirical orthogonal functions (EOFs), provide insight into the underlying geographical distribution of hydroclimatic variability (Figure 4). These EOFs capture spatially cohesive zones that correspond with different modes of climate forcing, and remain stable regardless of the specific time scale of SPEI used. As such, they offer a reliable basis for understanding the interaction between atmospheric dynamics and regional moisture conditions.

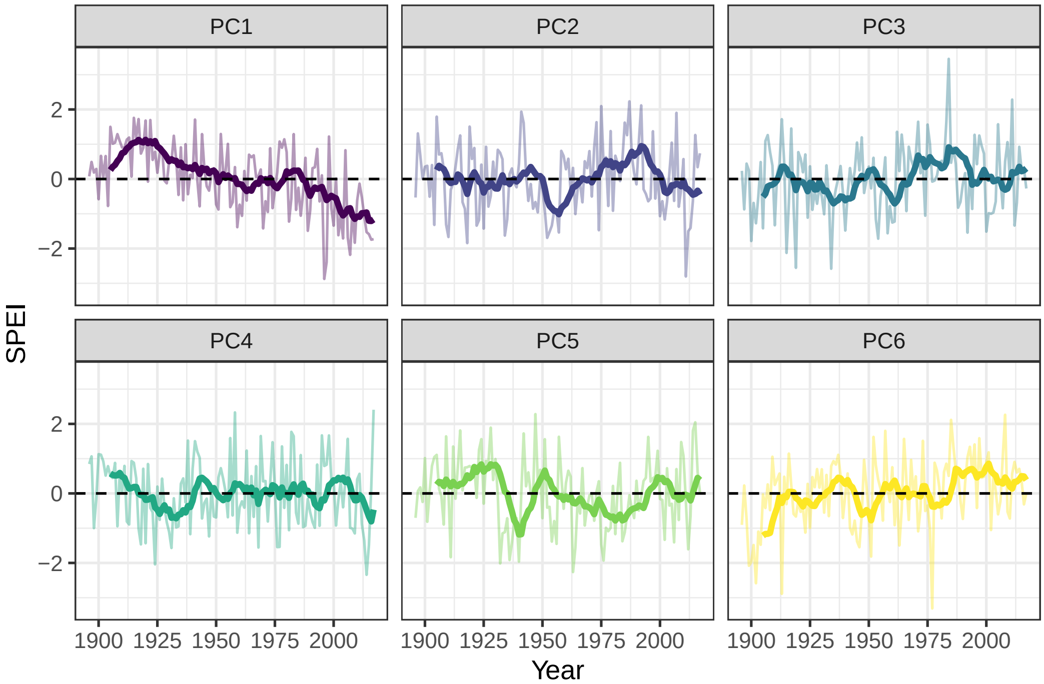

Figure 3. Time series associated with the leading 6 PCs for the observational period, after varimax rotation. SPEI values can be interpreted as z-scores in a normal distribution (i.e. a value of 1 is one standard deviation wetter than average for that location, -1 is one standard deviation drier). The dashed line corresponds to a SPEI value of 0 (i.e. average climatic water balance). 10 year moving averages superimposed over raw annual values. Observed PC time series are shown here to aid in interpretation of the underlying physical mechanisms, and all save PC6 are present in an independent SPEI reconstruction from the last millennium.

doi:10.20944/preprints202511.0803.v1

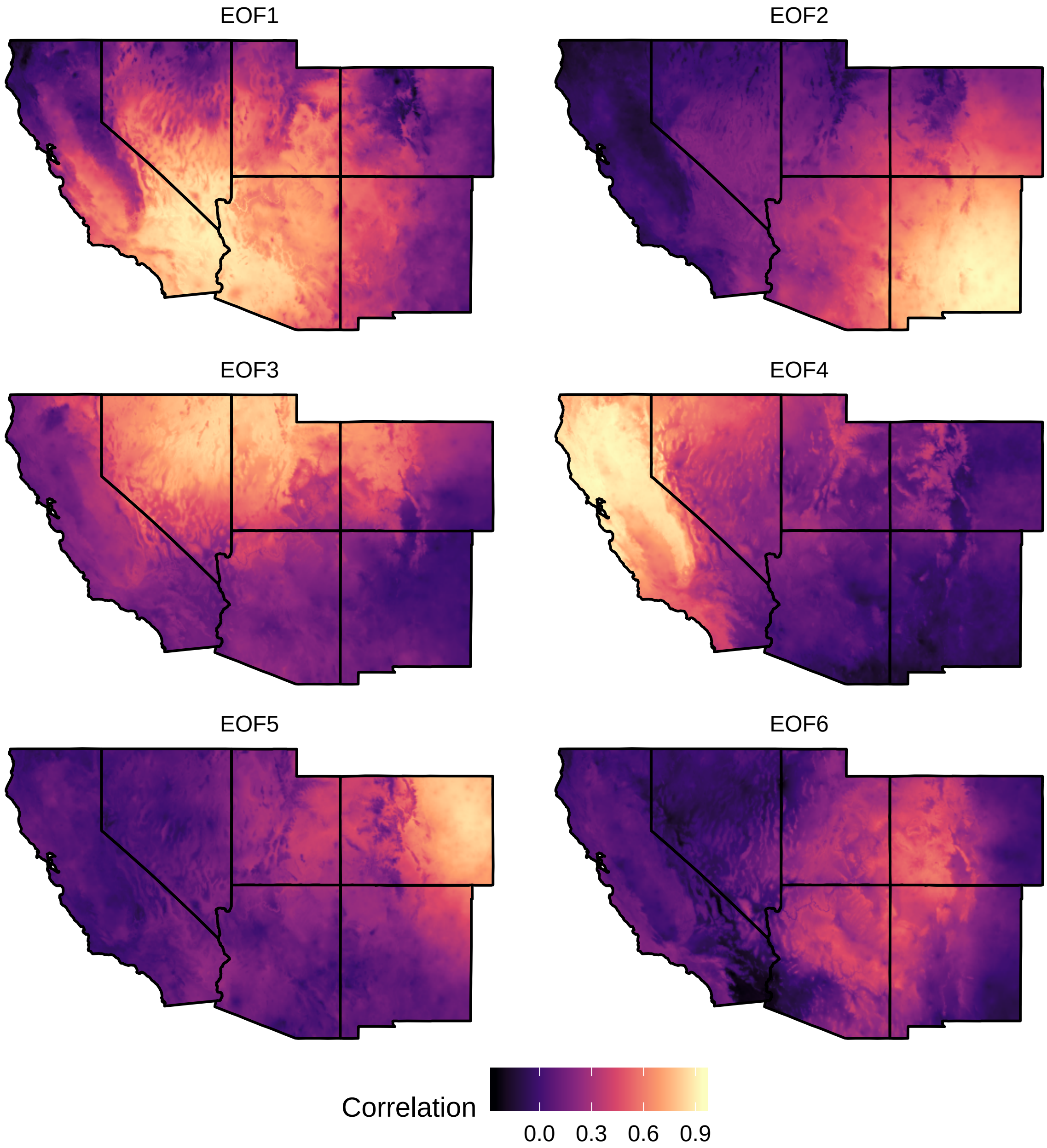

Figure 4. Leading 6 rotated empirical orthogonal functions (EOFs). The empirical orthogonal functions are the spatial patterns associated with their respective principal component time series in Figure 3. The EOFs are the eigenvectors of the space-time covariance matrix, and the PCs are the eigenvalues. The leading six EOFs, which together explain 77% of interannual drought variability in the observational record, were then subjected to varimax rotation, to make the spatial patterns more physically meaningful by relaxing the spatial orthogonality constraint.

Each EOF appears to correspond to a distinct pathway of moisture transport influenced by topographic and oceanic features. For example, EOF1 illustrates the impact of moisture-laden southwesterly flows originating from the tropical Pacific. This pattern is strongest in the lower elevation deserts of California and Arizona and weakens with increasing elevation and inland distance. The associated PC shows a persistent drying trend toward the present, likely linked to rising evaporative demand under recent warming.

 doi:10.20944/preprints202511.0803.v1

EOF2 captures the influence of humid air masses entering from the Gulf of Mexico and is centered on eastern New Mexico. Similar to EOF1, the signal declines with distance from the ocean, shaped by both terrain and continentality. PC2 reflects a historically severe drought in 1956 centered on the Texas–New Mexico region.

EOF3 indicates northerly continental air incursions, including cold fronts from polar sources, with its PC marked by wet anomalies such as those during the 1983 Salt Lake City floods. EOF4 captures the westerly influence from the Pacific and orographic interactions with the Sierra Nevada range—closely associated with events like the 1924 California drought and the Dust Bowl.

EOF5 is focused on the Great Plains and diminishes across the Rockies, strongly representing the Dust Bowl drought of the 1930s. Lastly, EOF6 centers on the Colorado Plateau and likely represents localized continental heating effects. Notably, this pattern is absent in lower-resolution paleoclimate reconstructions, suggesting it may be a product of more localized processes.

3.3. Climate and Distance Jointly Influence Social Connectivity

To understand how hydroclimate variability shaped patterns of social interaction, we first evaluated a baseline model in which geographic distance alone determines cultural similarity among archaeological sites. This null model, which represents a minimal assumption scenario, explains around 35% of the variation in ceramic assemblage similarity. As shown in Figure 5, interaction intensity declines substantially after 100 hours of modeled travel time, consistent with expectations from least-cost path analysis. Close geographic proximity remains a strong predictor of cultural interaction, though unexplained long-distance ties suggest additional structuring forces at play.

Building upon this foundation, we incorporated hydroclimatic differences between regions—quantified as the absolute difference in EOF loadings—into the spatial interaction model. This extended model increases the explained variance to approximately 41%. Though the improvement appears modest, it is statistically significant and consistent across multiple model selection criteria (AIC, BIC, and R^2).

The smooth functions estimated for each EOF term (Figure 6) show varying effects on interaction intensity. For some EOFs, increased climatic dissimilarity corresponds with heightened cultural similarity, supporting the hypothesis that trade or information exchange was preferentially maintained between regions experiencing contrasting drought regimes. In other cases, greater climatic differences are associated with diminished interaction, suggesting that climate divergence may inhibit connectivity under certain conditions.

doi:10.20944/preprints202511.0803.v1

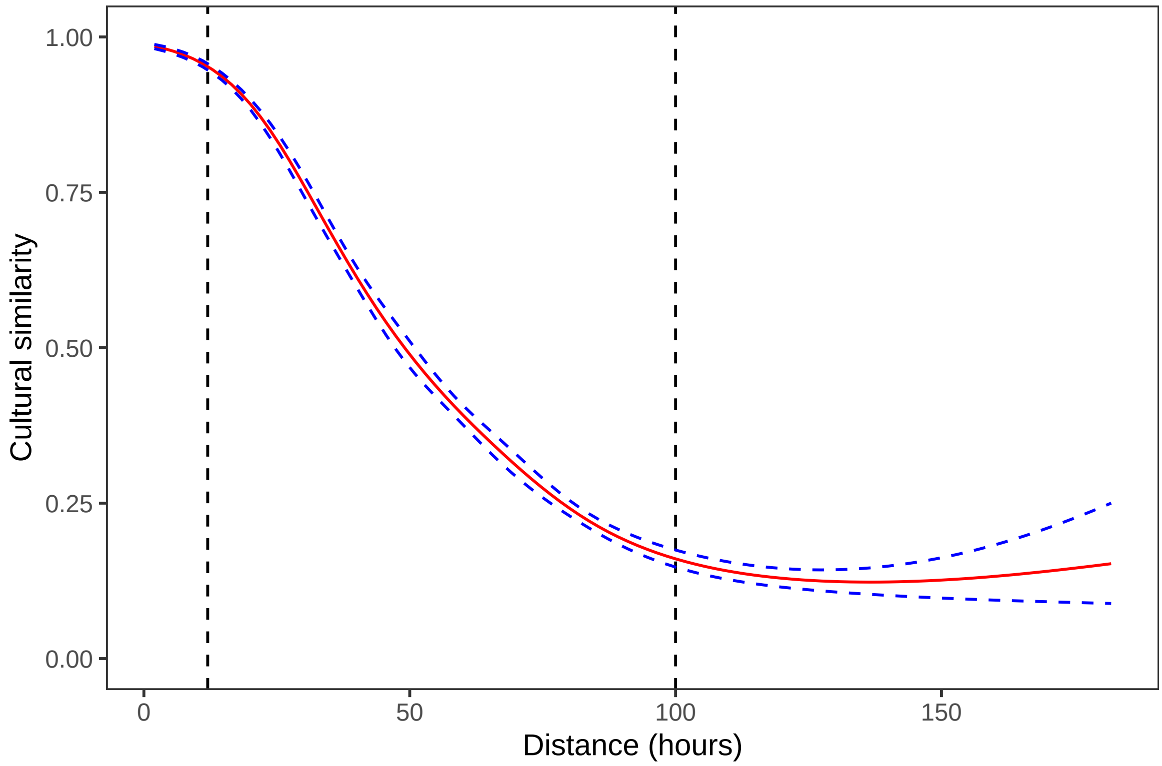

Figure 5. Empirical deterrence function showing how cultural similarity declines with distance between settlements, with thresholds at 10 and 100 hours.

Interestingly, several EOFs exert minimal influence, as indicated by nearly flat smoothing functions—a result of regularization during model fitting. Furthermore, effects do not systematically correspond to the sign or phase of the principal components over time, implying that climatic influence on social behavior may operate on complex, non-linear timescales extending beyond single-generation windows.

These results highlight the nuanced role of environmental heterogeneity in shaping the intensity and structure of social exchange networks. While distance remains a primary constraint, hydroclimate dynamics contribute a secondary yet significant layer of influence, particularly when examined at the regional scale and over extended temporal horizons.

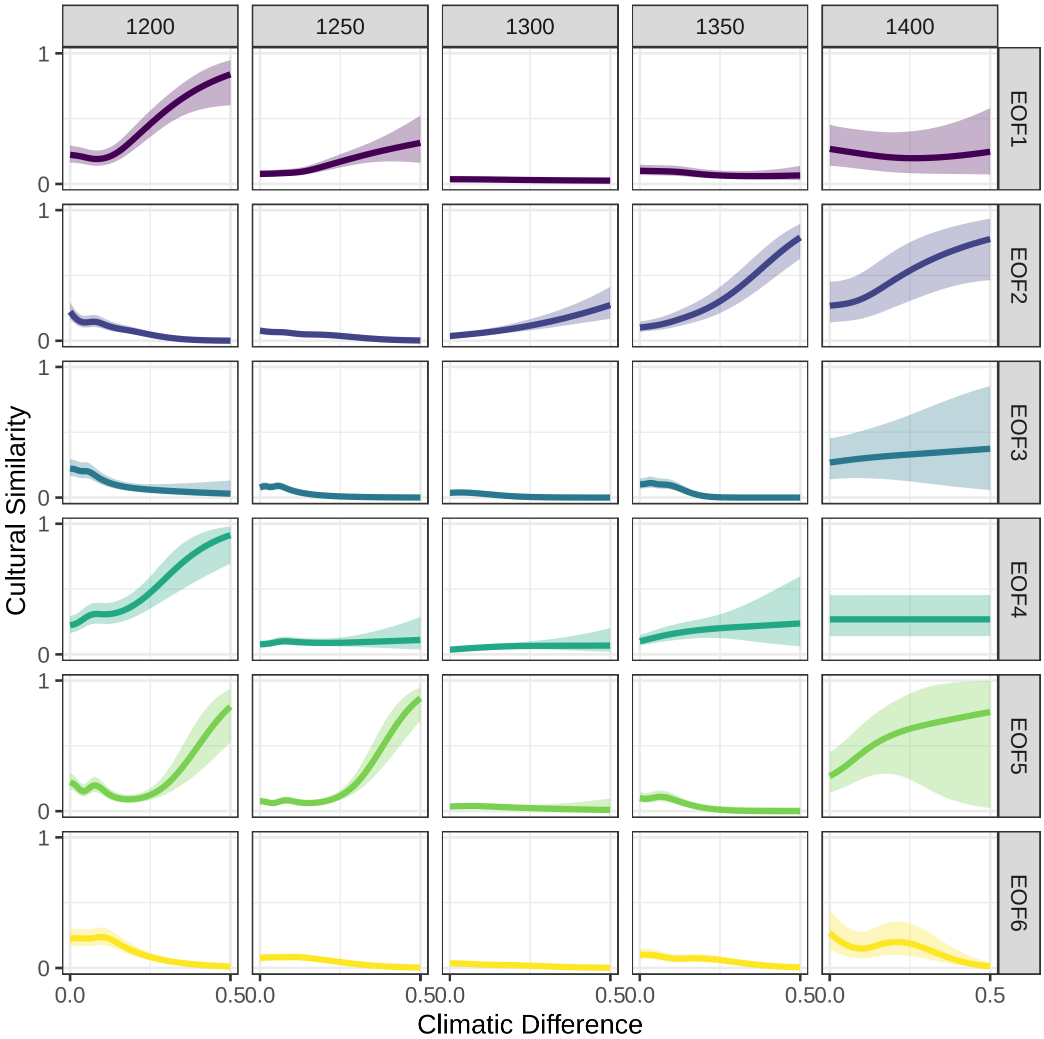

Figure 6. Estimated smooth functions showing how social interaction intensity varies with climatic distance across six drought patterns over five time periods.

4. Limitations and Future Work

While this study offers novel insights into the relationship between hydroclimate variability and social networks in the prehistoric American Southwest, several limitations should be acknowledged. First, the archaeological dataset, although extensive, does not capture the full spatial and temporal range of past human settlements and interactions. Preservation biases, survey coverage gaps, and uneven sampling intensity may influence the representativeness of the ceramic assemblages used to infer social connectivity.

Second, the temporal resolution of the social interaction proxies and climate reconstructions, aggregated into multi-decadal intervals, may obscure shorter-term dynamics and episodic events that shaped human responses. The reliance on ceramic similarity as a proxy for social interaction, while powerful, cannot fully capture the complexity of exchange mechanisms, including non-material transfers such as knowledge, rituals, or political alliances.

Third, the spatial interaction models employed assume stationarity and equilibrium conditions that may not reflect the adaptive, non-linear nature of human social systems. For example, social networks may undergo rapid reorganization during environmental crises or sociopolitical upheavals, which are challenging to detect in averaged data.

Future research could address these constraints through several avenues. Incorporating high-resolution paleoclimate proxies and archaeological data would enable finer temporal and spatial analysis of climate-society dynamics. Agent-based modeling and simulation approaches could offer

 doi:10.20944/preprints202511.0803.v1

a mechanistic understanding of how social networks evolve under environmental stress, explicitly modeling feedbacks, network resilience, and collapse scenarios. Additionally, integrating ethnographic and oral histories of contemporary dryland communities could provide analogues to better interpret archaeological patterns and inform models of human adaptation.

Continued efforts to digitize and standardize archaeological datasets across regions would also facilitate comparative studies, enabling a broader evaluation of how diverse societies responded to similar climatic challenges. Overall, advancing interdisciplinary collaborations between archaeologists, climatologists, and social scientists will be critical to refining our understanding of the complex interplay between environment and society over long timescales.

5. Implications for Contemporary Climate Adaptation

The findings from this study hold important lessons for contemporary societies facing increasing climate variability and environmental stress. Prehistoric exchange networks in arid landscapes developed as adaptive strategies to manage risk and uncertainty associated with fluctuating water availability. These networks provided social infrastructure essential for resource sharing, information flow, and cooperative resilience in the face of drought.

Modern smallholder farmers and rural communities in drylands around the world similarly depend on complex social and economic networks to navigate climatic challenges. Understanding the conditions under which ancient social systems succeeded or failed can inform current efforts to enhance community resilience. For instance, the fragility of past exchange networks under unprecedented drought conditions highlights the need for institutional flexibility and the diversification of social ties in contemporary adaptation strategies.

Moreover, the role of spatial climate variability in structuring social interactions underscores the value of fostering interregional cooperation between ecologically distinct areas. Just as prehistoric populations maintained ties across diverse hydroclimatic zones to mitigate localized stress, modern adaptation policies might benefit from promoting cross-regional collaboration in resource management, knowledge exchange, and disaster preparedness.

Finally, the persistence of hierarchical social structures observed archaeologically suggests that power dynamics and governance play a critical role in shaping adaptive capacity. Contemporary adaptation planning should consider how social equity, inclusion, and local leadership influence the robustness of social networks under climate stress.

By integrating insights from archaeological studies of past human-environment interactions, policymakers, development practitioners, and communities can design more informed and culturally sensitive adaptation interventions, ultimately contributing to sustainable livelihoods in the face of accelerating global climate change.

6. Discussion and Conclusions

The six dominant hydroclimate patterns identified in this study align with well-established climatic mechanisms in the American Southwest, each reflecting distinct pathways of moisture transport shaped by both topography and oceanic influences [63,64]. These spatial modes are robust across multiple datasets and timescales, appearing not only in observational records but also in paleoclimate reconstructions [13,15,65]. This consistency supports their relevance for interpreting long-term environmental dynamics.

By using objective measures of spatial drought variability, we move beyond simplistic point comparisons and capture underlying climatic structures that better explain regional social behavior. The strongest climatic drivers of interaction appear to be those associated with Pacific and Atlantic sea surface temperature variability [15]. Major social disruptions in the archaeological record coincide with departures from these usual climate patterns, suggesting that environmental unpredictability challenged the adaptability of existing exchange systems [28].

The analysis reveals that while geographic proximity remains a key factor in social connectivity, hydroclimatic differences also play a meaningful role. Interestingly, not all climatic dissimilarity promotes exchange—some patterns seem to facilitate connections, while others inhibit them. This implies a complex relationship shaped by ecological conditions, sociopolitical organization, and perhaps ethnolinguistic identity [4,66]. Exchange may have been mediated through elite or hierarchical structures not fully captured in basic network models.

Unexplained residual structure in the models hints at persistent cultural clusters and local patterns of transitive ties. These may stem from mechanisms like kinship-based interactions or network closure, which require more specialized modeling approaches [67]. Moreover, limitations in spatial data coverage restrict our ability to test the full range of climatic variation and introduce uncertainty in distinguishing among overlapping environmental influences [62].

Beyond archaeology, these findings highlight the broader relevance of climate-linked social networks. As in the past, present-day smallholder farming communities rely on intricate social systems to navigate environmental stress. The historical persistence of such networks, shaped by long-term climatic patterns, underscores the need to design institutions today that can adapt to changing variability [68]. Insights from the past may offer valuable guidance for enhancing resilience in contemporary social-ecological systems facing climate change.

References

1. Anderies, J.M. Understanding the Dynamics of Sustainable Social-Ecological Systems: Human Behavior, Institutions, and Regulatory Feedback Networks. *Bulletin of Mathematical Biology* **2015**, *77*, 259–280. https://doi.org/10.1007/s11538-014-0030-z.
2. Fafchamps, M.; Gubert, F. The formation of risk sharing networks. *Journal of Development Economics* **2007**, *83*, 326–350. https://doi.org/10.1016/j.jdeveco.2006.05.005.
3. Bloch, F.; Genicot, G.; Ray, D. Informal insurance in social networks. *Journal of Economic Theory* **2008**, *143*, 36–58. https://doi.org/10.1016/j.jet.2008.01.008.
4. Nolin, D.A. Food-Sharing Networks in Lamalera, Indonesia. *Human Nature* **2010**, *21*, 243–268. https://doi.org/10.1007/s12110-010-9091-3.
5. Verdery, A.M.; Entwisle, B.; Faust, K.; Rindfuss, R.R. Social and spatial networks: Kinship distance and dwelling unit proximity in rural Thailand. *Social Networks* **2012**, *34*, 112–127, [NIHMS150003]. https://doi.org/10.1016/j.socnet.2011.04.003.
6. Freeman, J.; Anderies, J.M.; Torvinen, A.; Nelson, B.A. Crop Specialization, Exchange and Robustness in a Semi-arid Environment. *Human Ecology* **2014**, *42*, 297–310. https://doi.org/10.1007/s10745-013-9638-0.
7. Koster, J.M.; Leckie, G. Food sharing networks in lowland Nicaragua: An application of the social relations model to count data. *Social Networks* **2014**, *38*, 100–110. https://doi.org/10.1016/j.socnet.2014.02.002.
8. Hao, Y.; Armbruster, D.; Cronk, L.; Aktipis, C.A. Need-based transfers on a network: A model of risk-pooling in ecologically volatile environments. *Evolution and Human Behavior* **2015**, *36*, 265–273. https://doi.org/10.1016/j.evolhumbehav.2014.12.003.
9. Schnegg, M. Reciprocity on Demand: Sharing and Exchanging Food in Northwestern Namibia. *Human Nature* **2015**, *26*, 313–330. https://doi.org/10.1007/s12110-015-9236-5.
10. Rautman, A.E. Resource Variability, Risk, and the Structure of Social Networks: An Example from the Prehistoric Southwest. *American Antiquity* **1993**, *58*, 403–424.
11. Durante, R. Risk, Cooperation and the Economic Origins of Social Trust: An Empirical Investigation. https://doi.org/10.2139/ssrn.1576774.
12. Halstead, P.; O'Shea, J. Introduction: cultural responses to risk and uncertainty. In *Bad Year Economics: Cultural Responses to Risk and Uncertainty*; Halstead, P.; O'Shea, J., Eds.; Cambridge University Press: Cambridge, 1989; chapter 1, pp. 1–7. https://doi.org/10.2307/281441.
13. Cook, E.R.; Meko, D.M.; Stahle, D.W.; Cleaveland, M.K. Drought reconstructions for the continental United States. *Journal of Climate* **1999**, *12*, 1145–1163. https://doi.org/10.1175/1520-0442(1999)012<1145:DRFTCU>2.0.CO;2.
14. Sheppard, P.R.; Comrie, A.C.; Packin, G.D.; Angersbach, K.; Hughes, M.K. The Climate of the US Southwest. *Climate Research* **2002**, *21*, 219–238. https://doi.org/10.3354/cr021219.

15. McCabe, G.J.; Palecki, M.A.; Betancourt, J.L. Pacific and Atlantic Ocean influences on multidecadal drought frequency in the United States. *Proceedings of the National Academy of Sciences* **2004**, *101*, 4136–4141, [arXiv:10.1002/2014WR016527]. https://doi.org/10.1073/pnas.0306738101.
16. Herweijer, C.; Seager, R.; Cook, E.R.; Emile-Geay, J. North American Droughts of the Last Millennium from a Gridded Network of Tree-Ring Data. *Journal of Climate* **2007**, *20*, 1353–1376. https://doi.org/10.1175/JCLI4042.1.
17. Cook, B.I.; Cook, E.R.; Anchukaitis, K.J.; Seager, R.; Miller, R.L. Forced and unforced variability of twentieth century North American droughts and pluvials. *Climate Dynamics* **2011**, *37*, 1097–1110. https://doi.org/10.1007/s00382-010-0897-9.
18. Bocinsky, R.K.; Kohler, T.A. A 2,000-year reconstruction of the rain-fed maize agricultural niche in the US Southwest. *Nature Communications* **2014**, *5*, 5618. https://doi.org/10.1038/ncomms6618.
19. Coats, S.; Smerdon, J.E.; Cook, B.I.; Seager, R. Are Simulated Megadroughts in the North American Southwest Forced? *Journal of Climate* **2015**, *28*, 124–142. https://doi.org/10.1175/JCLI-D-14-00071.1.
20. Routson, C.C.; Woodhouse, C.A.; Overpeck, J.T.; Betancourt, J.L.; McKay, N.P. Teleconnected ocean forcing of Western North American droughts and pluvials during the last millennium. *Quaternary Science Reviews* **2016**, *146*, 238–250. https://doi.org/10.1016/j.quascirev.2016.06.017.
21. Ault, T.R.; George, S.S.; Smerdon, J.E.; Coats, S.; Mankin, J.S.; Carrillo, C.M.; Cook, B.I.; Stevensong, S. A robust null hypothesis for the potential causes of megadrought in Western North America. *Journal of Climate* **2018**, *31*, 3–24. https://doi.org/10.1175/JCLI-D-17-0154.1.
22. Hill, J.B.; Clark, J.J.; Doelle, W.H.; Lyons, P.D. Prehistoric Demography in the Southwest: Migration, Coalescence, and Hohokam Population Decline. *American Antiquity* **2004**, *69*, 689–716. https://doi.org/10.2307/4128444.
23. Malville, N.J. Long-Distance Transport of Bulk Goods in the Pre-Hispanic American Southwest. *Journal of Anthropological Archaeology* **2001**, *20*, 230–243. https://doi.org/10.1006/jaar.2000.0373.
24. Taliaferro, M.S.; Schriever, B.A.; Shackley, M.S. Obsidian procurement, least cost path analysis, and social interaction in the Mimbres area of southwestern New Mexico. *Journal of Archaeological Science* **2010**, *37*, 536–548. https://doi.org/10.1016/j.jas.2009.10.018.
25. Mills, B.J.; Clark, J.J.; Peeples, M.a.; Haas, W.R.; Roberts, J.M.; Hill, J.B.; Huntley, D.L.; Borck, L.; Breiger, R.L.; Clauset, A.; et al. Transformation of social networks in the late pre-Hispanic US Southwest. *Proceedings of the National Academy of Sciences of the United States of America* **2013**, *110*, 5785–90. https://doi.org/10.1073/pnas.1219966110.
26. Benson, L.V.; Stein, J.R.; Taylor, H.E. Possible sources of archaeological maize found in Chaco Canyon and Aztec Ruin, New Mexico. *Journal of Archaeological Science* **2009**, *36*, 387–407. https://doi.org/10.1016/j.jas.2008.09.023.
27. Benson, L.V. Who provided maize to Chaco Canyon after the mid-12th-century drought? *Journal of Archaeological Science* **2010**, *37*, 621–629. https://doi.org/10.1016/j.jas.2009.10.027.
28. Cordell, L.S.; Van West, C.R.; Dean, J.S.; Muenchrath, D.A. Mesa Verde settlement history and relocation: Climate change, social networks, and Ancenstral Pueblo migration. *Kiva* **2007**, *72*, 379–405. https://doi.org/10.1179/kiv.2007.72.4.001.
29. Strawhacker, C.; Snitker, G.; Spielmann, K.A.; Wasiolek, M.; Sandor, J.; Kinzig, A.; Kintigh, K. Risk landscapes and domesticated landscapes: Food Security in the Salinas province. In *Landscapes of Social Transformation in the Salinas Province and the Eastern Pueblo World*; Spielmann, K.A., Ed.; University of Arizona Press, 2017; pp. 103–118. https://doi.org/10.2307/j.ctt1tp3c7x.7.
30. Borck, L.; Mills, B.J.; Peeples, M.A.; Clark, J.J. Are Social Networks Survival Networks? An Example from the Late Pre-Hispanic US Southwest. *Journal of Archaeological Method and Theory* **2015**, *22*, 33–57. https://doi.org/10.1007/s10816-014-9236-5.
31. Lorenz, E.N. Empirical Orthogonal Functions and Statistical Weather Prediction. Technical Report Scientific Report No. 1, Statistical Forecasting Project, 1956.
32. Hannachi, A.; Jolliffe, I.T.; Stephenson, D.B. Empirical orthogonal functions and related techniques in atmospheric science: A review. *International Journal of Climatology* **2007**, *27*, 1119–1152. https://doi.org/10.1002/joc.1499.
33. Weiss, B. The decline of Late Bronze Age civilization as a possible response to climatic change. *Climatic Change* **1982**, *4*, 173–198. https://doi.org/10.1007/BF02423389.
34. Daly, C.; Taylor, G.; Gibson, W. The Prism Approach to Mapping Precipitation and Temperature. *10th AMS Conference on Applied Climatology* **1997**, pp. 1–4.

35. Vicente-Serrano, S.M.; Beguería, S.; López-Moreno, J.I.; Angulo, M.; El Kenawy, A. A New Global 0.5° Gridded Dataset (1901–2006) of a Multiscalar Drought Index: Comparison with Current Drought Index Datasets Based on the Palmer Drought Severity Index. *Journal of Hydrometeorology* **2010**, *11*, 1033–1043. https://doi.org/10.1175/2010JHM1224.1.
36. North, G.R.; Bell, T.L.; Cahalan, R.F. Sampling Errors in the Estimation of Empirical Orthogonal Funtions, 1982. https://doi.org/10.1175/1520-0493(1982)110<0699:SEITEO>2.0.CO;2.
37. Richman, M.B. Review Article: Rotation of principal components. *Journal of Climatology* **1986**, *6*, 293–335. https://doi.org/10.1056/NEJMra1313875.
38. Steiger, N.J.; Smerdon, J.E.; Cook, E.R.; Cook, B.I. A reconstruction of global hydroclimate and dynamical variables over the Common Era. *Scientific Data* **2018**, *5*, 1–15. https://doi.org/10.1038/sdata.2018.86.
39. Mills, B.J.; Roberts Jr, J.M.; Clark, J.J.; Haas Jr, W.R.; Huntley, D.; Peeples, M.A.; Borck, L.; Ryan, S.C.; Trowbridge, M.; Breiger, R.L. The Dynamics of Social Networks in the Late Prehispanic US Southwest. In *Network analysis in archaeology: New approaches to regional interaction*; Oxford University Press, 2013; chapter 8, pp. 181–202.
40. Peeples, M.A.; Haas, W.R. Brokerage and Social Capital in the Prehispanic U.S. Southwest. *American Anthropologist* **2013**, *115*, 232–247. https://doi.org/10.1111/aman.12006.
41. Hill, J.B.; Peeples, M.A.; Huntley, D.L.; Carmack, H.J. Spatializing Social Network Analysis in the Late Precontact U.S. Southwest. *Advances in Archaeological Practice* **2015**, *3*, 63–77. https://doi.org/10.7183/2326-3768.3.1.63.
42. Mills, B.J.; Peeples, M.A.; Haas, Jr., W.R.; Borck, L.; Clark, J.J.; Roberts, Jr., J.M. Multiscalar Perspectives on Social Networks in the Late Prehispanic Southwest. *American Antiquity* **2015**, *80*, 3–24. https://doi.org/10.7183/0002-7316.79.4.3.
43. Paliou, E.; Bevan, A. Evolving settlement patterns, spatial interaction and the socio-political organisation of late Prepalatial south-central Crete. *Journal of Anthropological Archaeology* **2016**, *42*, 184–197. https://doi.org/10.1016/j.jaa.2016.04.006.
44. Masucci, A.P.; Kalampokis, A.; Eguíluz, V.M.; Hernández-García, E. Wikipedia information flow analysis reveals the scale-free architecture of the semantic space. *PLoS ONE* **2011**, *6*, e17333, [1102.0651]. https://doi.org/10.1371/journal.pone.0017333.
45. Anderies, J.M.; Hegmon, M. Robustness and Resilience Across Scales: Migration and Resource Degradation in the Prehistoric US Southwest. *Ecology and Society* **2011**, *16*, 22. https://doi.org/22.
46. Drennan, R.D. Long-distance transport costs in pre-Hispanic Mesoamerica. *American Anthropologist* **1984**, *86*, 105–112.
47. Pingel, T.J. Modeling Slope as a Contributor to Route Selection in Mountainous Areas. *Cartography and Geographic Information Science* **2010**, *37*, 137–148. https://doi.org/10.1559/152304010791232163.
48. van Etten, J. R Package gdistance: Distances and Routes on Geographical Grids. *Journal of Statistical Software* **2014**, *59*.
49. Wilson, A. Family of spatial interaction models, and associated developments. *Environment and Planning* **1971**, *3*, 1–32. https://doi.org/10.1068/a030001.
50. Fotheringham, S.A.; O'Kelly, M.E. *Spatial interaction models: formulations and applications*; Kluwer Academic Publishers, 1989.
51. Sen, A.; Smith, T.E. *Gravity Models of Spatial Interaction Behavior*; Springer-Verlag, 1995; p. 572.
52. Bavaud, F. The endogenous analysis of flows, with applications to migrations, social mobility and opinion shifts. *Journal of Mathematical Sociology* **2008**, *32*, 239–266. https://doi.org/10.1080/00222500802352493.
53. Murphy, M.A.; Dezzani, R.; Pilliod, D.S.; Storfer, A. Landscape genetics of high mountain frog metapopulations. *Molecular Ecology* **2010**, *19*, 3634–3649. https://doi.org/10.1111/j.1365-294X.2010.04723.x.
54. Head, K.; Mayer, T. *Gravity Equations: Workhorse,Toolkit, and Cookbook*; Vol. 4, Elsevier B.V., 2015; pp. 131–195. https://doi.org/10.1016/B978-0-444-54314-1.00003-3.
55. Tobler, W.; Wineburg, S. A cappadocian speculation. *Nature* **1971**, *231*, 39–41. https://doi.org/10.1038/231039a0.
56. Hodder, I. Regression analysis of some trade and marketing patterns. *World Archaeology* **1974**, *6*, 172–189. https://doi.org/10.1080/00438243.1974.9979600.
57. Johnson, J.R. Chumash social geography: A quantitative analysis. *Proceedings of the Society of California Archaeology* **1990**, *3*, 149–173.
58. Mesoudi, A. Migration, acculturation, and the maintenance of between-group cultural variation. *PLoS ONE* **2018**, *13*, 1–23. https://doi.org/https://doi.org/10.1371/journal.pone.0205573Editor:.

doi:10.20944/preprints202511.0803.v1

59. Wood, S.N. *Generalized Additive Models: An Introduction with R*; Chapman and Hall/CRC press, 2006. https://doi.org/10.1111/j.1541-0420.2006.00574.x.
60. Lebacher, M.; Thurner, P.W.; Kauermann, G. International Arms Trade: A Dynamic Separable Network Model With Heterogeneity Components **2018**. [1803.02707].
61. Clarke, R.T.; Rothery, P.; Raybould, A.F. Confidence Limits for Regression Relationships Between Distance Matrices : Estimating Gene Flow With Distance. *Journal of Agricultural, Biological, and Environmental Statistics* **2002**, *7*, 361–372. https://doi.org/10.1198/108571102320.
62. Shirk, A.J.; Landguth, E.L.; Cushman, S.A. A comparison of regression methods for model selection in individual-based landscape genetic analysis. *Molecular Ecology Resources* **2018**, *18*, 55–67, [arXiv:arXiv:physics/0608246v3]. https://doi.org/10.1111/1755-0998.12709.
63. Liu, Z.; Bowen, G.J.; Welker, J.M. Atmospheric circulation is reflected in precipitation isotope gradients over the conterminous United States. *Journal of Geophysical Research Atmospheres* **2010**, *115*, 1–14. https://doi.org/10.1029/2010JD014175.
64. Hu, Q.; Feng, S.; Oglesby, R.J. Variations in North American summer precipitation driven by the Atlantic multidecadal oscillation. *Journal of Climate* **2011**, *24*, 5555–5570. https://doi.org/10.1175/2011JCLI4060.1.
65. Seager, R.; Hoerling, M. Atmosphere and ocean origins of North American droughts. *Journal of Climate* **2014**, *27*, 4581–4606. https://doi.org/10.1175/JCLI-D-13-00329.1.
66. Crumley, C.L. *Three Locational Models: An Epistemological Assessment for Anthropology and Archaeology*; Vol. 2, 1979; pp. 141–173.
67. Stillman, P.E.; Wilson, J.D.; Denny, M.J.; Desmarais, B.A.; Bhamidi, S.; Cranmer, S.J.; Lu, Z.L. Statistical Modeling of the Default Mode Brain Network Reveals a Segregated Highway Structure. *Scientific Reports* **2017**, *7*, 1–14, [arXiv:1408.1149]. https://doi.org/10.1038/s41598-017-09896-6.
68. Janssen, M.A.; Anderies, J.M.; Ostrom, E. Robustness of Social-Ecological Systems to Spatial and Temporal Variability. *Society & Natural Resources* **2007**, *20*, 307–322. https://doi.org/10.1080/08941920601161320.